The HEAO-2 Guest Investigator Program:

# NON-LINEAR GROWTH OF INSTABILITIES IN LINE-DRIVEN STELLAR WINDS

Grant NAG 8-463

Semiannual Progress Report No. 3

For the period 1 November 1984 through 30 April 1985


Principal Investigator

George B. Rybicki

August 1985

Prepared for
National Aeronautics and Space Administration
Marshall Space Flight Center, AL 35812

Smithsonian Institution
Astrophysical Observatory
Cambridge, Massachusetts 02138



The Smithsonian Astrophysical Observatory
is a member of the
Harvard-Smithsonian Center for Astrophysics

The NASA Technical Officer for this grant is Dr. W. G. Johnson, Marshall Space Flight Center, AL 35812.

The HEAO-2 Guest Investigator Program:

# NON-LINEAR GROWTH OF INSTABILITIES IN LINE-DRIVEN STELLAR WINDS

Grant NAG 8-463

Semiannual Progress Report No. 3

For the period 1 November 1984 through 30 April 1985

Principal Investigator

George B. Rybicki

August 1985

Prepared for
National Aeronautics and Space Administration
Marshall Space Flight Center, AL 35812

Smithsonian Institution
Astrophysical Observatory
Cambridge, Massachusetts 02138



The NASA Technical Officer for this grant is Dr. W. G. Johnson, Marshall Space Flight Center, AL 35812.

During this reporting period we have continued to investigate the instability discussed in Owocki and Rybicki (1984, Ap. J., 284, 337; paper I). A second paper was submitted for publication describing the effects of line scattering and line overlap on the instability. This paper upholds our earlier conclusion that hot stellar winds are highly unstable to the growth of short wavelength perturbations, and it is very likely that formation and dissapation of shocks will occur and will be responsible for the heating of the winds to observed X-ray temperatures.

Further work has been done on the problem of wave propagation in hot stellar winds. Numerical studies of pulse propagation have been undertaken in order to understand better the precise nature of the instability and the nature of information flows within the wind, which are important for understanding the critical point conditions that determine the properties of such winds, especially the mass loss rates. We have shown in the case of pure absorption line driving that the inward propagation of information occurs at the sound speed and not at the supersonic speed described by Abbott (1980; Astrophys. Journ. 240, 1183). It is not yet clear what the effective speed of information will be under conditions of pure line scattering.

Publications:

Owocki, S.P., and Rybicki, G.B. Effect of Scattering on Instabilities in Line-Driven Stellar Winds. Proceedings of the Colloquium/Workshop on The Origin of Non-Radiative Heating/Momentum in Hot Stars, held at Goddard SFC, 5-7 June 1984. NASA Conference Publication 2358 (1985).

Papers submitted:

Owocki, S.P., and Rybicki, G.B. Instabilities in Line-Drive Stellar Winds: II. Effects of Scattering. Submitted to Astrophysical Journal, 25 March 1985.

Papers in preparation:

Rybicki, G.B., and Owocki, S.P. Wave Propagation in Stellar Winds Driven by Pure Line Absorption. To be submitted to Astrophysical Journal.

Presentations at Meetings and Conferences:

Rybicki, G.B., and Owocki, S.P. Effect of Scattering on the Instability of Radiation-Driven Stellar Winds, presented at the 165th Meeting of the AAS, Tucson, Arizona, 13-16 January 1985. Abstract published in BAAS, 16, 993 (1984).

SP-85-03

# INSTABILITIES IN LINE-DRIVEN STELLAR WINDS: II. EFFECT OF SCATTERING

S.P. Owocki

Center for Astrophysics and Space Sciences,

University of California at San Diego

G.B. Rybicki

Harvard-Smithsonian Center for Astrophysics

Received: _____

Submitted to The Astrophysical Journal

ABSTRACT

We extend our earlier analysis (Owocki and Rybicki 1984; paper I) of the linear instability of line-driven stellar winds to take proper account of the dynamical effect of scattered radiation. The principal differences from the previous study of scattering by Lucy (1984) are: 1) We use the physically more reasonable assumptions of complete redistribution (vs. coherent scattering) and spherically symmetric (vs. plane parallel) flow in the wind. 2) In addition to examining Lucy's "drag effect" of the *mean* scattered radiation field on velocity perturbations, we also investigate the role of *perturbations* in the scattered field itself. 3) We quantitatively examine the effects of line overlap.

Our principal findings are: 1) The drag effect of the mean scattered radiation does indeed greatly reduce the contribution of scattering lines to the instability at the very base of the wind, but the instability growth rate associated with such lines rapidly increases as the flow moves outward from the base, reaching more than 50% of the growth rate for pure absorption lines within a stellar radius of the surface, and eventually reaching 80% of that rate at large radii. 2) Perturbations in the scattered radiation field may be important for the propagation of wind disturbances, but they have little effect on the wind instability. 3) The contribution of strongly shadowed lines to the wind instability is often reduced compared to that of unshadowed lines, but their overall effect is not (as suggested by Lucy 1984) one of damping in the outer parts of the wind.

The primary conclusion we derive from these results is thus that, even when all scattering effects are taken into account, the bulk of the flow in a line-driven stellar wind is still highly unstable.

# I. INTRODUCTION

In the first paper of this series (Owocki and Rybicki 1984; paper I), we showed that a flow driven by line absorption of a point source of continuum radiation is unstable to a velocity perturbation with a wavelength $\lambda$ approximately equal to or less than a Sobolev length $L$ (over which the mean flow velocity increases by a thermal speed), but becomes asymptotically stable to perturbations with $\lambda \gg L$. We thereby reconciled conclusions of the many earlier studies that had also found such flows unstable (Milne 1926; Lucy and Solomon 1970; Carlberg 1980; MacGregor, Hartmann, and Raymond 1980, hereafter MHR) with the work of Abbott (1980), who found them to be marginally stable. From this analysis, we then argued that the winds of hot, luminous, early-type (i.e., spectral classes O and B) stars, which are thought to be driven by line-absorption of the star's continuum radiative momentum flux (Lucy and Solomon 1970; Castor, Abbott, and Klein 1975, hereafter CAK; Cassinelli 1979; Abbott 1980, 1982; Cassinelli and MacGregor 1985; Abbott and Lucy 1985), are unstable to short wavelength perturbations.

Such winds are actually driven mostly by strong scattering (vs. pure absorption) lines (Abbott 1980; Abbott and Lucy 1984), but, in the supersonic portions of the wind, the scattered radiation can be shown (Sobolev 1957, 1960; Castor 1970, 1974; Lucy 1971) to have negligible dynamical effect on the mean flow in comparison with the direct "core" radiation from the stellar photosphere. On this basis, we argued in paper I that the scattered radiation field should have negligible dynamical effect on the *perturbed* flow as well, and hence that an analysis based solely on the extinction (i.e., neglecting scattering) of the core radiation would suffice to study the stability of the wind. Subsequently, Lucy (1984) criticized this neglect of scattering and showed that the mean scattered radiation field exerts a drag force on velocity perturbations which counteracts the amplifying effect of the force associated with the direct extinction of the core radiation. Under the specialized assumption that the scattering is coherent, Lucy found that this drag effect *exactly cancels* the contribution of isolated, pure scattering lines to the instability near the wind base, where the flow is nearly plane-parallel. He further conjectured that "in the outer parts of winds, line drag results in a damping contribution from resonance lines that are strongly shadowed by neighboring resonance transitions", and he thereby concluded that "line-driven winds would seem therefore not to be as highly unstable as hitherto claimed".

In order to examine this question of the effect of scattering lines on the stability of radiatively driven stellar winds, we have extended the analysis of paper I to take proper account of the dynamical effects of scattered radiation. Our analysis (§II and §III) differs from Lucy's in that it is based on the physically more reasonable assumptions that the scattering occurs with complete redistribution (vs. complete coherence) and that the mean wind flow is spherically symmetric (vs. plane parallel); further, in addition to Lucy's drag effect of the *mean* scattered field on velocity perturbations, we include the effects of *perturbations* in the scattered field itself. We also examine the effects of photospheric limb darkening (§IVa), photon destruction (§IVb), and line overlap (i.e., line shadowing; §IVc). The results (summarized in

§V) of this more complete scattering analysis lead to markedly different conclusions about the importance of scattering effects in reducing the instability of radiatively driven stellar winds. In particular, our primary conclusion is that, even when all line scattering effects (including line drag and line overlap) are taken into account, the bulk of the wind flow is still very unstable, a conclusion that is in agreement with that of paper I and in contradiction with that of Lucy (1984).

## II. PERTURBATION ANALYSIS FOR A SCATTERING LINE

### *a) Assumptions*

In examining line-driven stellar winds for stability against perturbations, it is important to calculate correctly the perturbed value of the line force. In this section, we calculate this perturbed line-force under the following assumptions:

1) The line is a *pure* scattering line so that the photon destruction probability per scattering $\epsilon = 0$.

2) The line is *isolated* so that its line center frequency is displaced from its nearest (blueward) neighbor by a velocity separation $\Delta v > 2v_\infty$, where $v_\infty$ is the asymptotic wind speed.

3) The line is optically thick, but unsaturated in the mean flow, so that scattering occurs in the Doppler core of the Voigt profile. We therefore ignore the line wings.

4) The line scattering is *isotropic*.

5) The line scattering occurs with *complete redistribution* in frequency.

6) The radiation from the underlying stellar photosphere is not limb darkened.

7) The mean wind flow is *radially directed* and *spherically symmetric*.

8) The wind is highly *supersonic* so that the mean flow speed $v_0 \gg v_{th}$ (where $v_{th}$ is the ion thermal speed), implying that the Sobolev approximation, $L \equiv v_{th}/v_0' \ll v_0/v_0' \equiv H$ ($\approx R_*$, the stellar radius), is satisfied for the mean flow.

9) Perturbations in the line opacity $\kappa$ can be ignored.

10) The perturbations are of the radial, sinusoidal form $\exp(i(kr - \omega t))$ with frequency $\omega$ and wavenumber $k$.

11) The perturbation wavelength $\lambda \ll R_*$ so that a WKB analysis is justified.

12) The perturbations are small amplitude so that a *linear* analysis is justified.

The effect of relaxing assumption (3) has already been examined in paper I, where we showed that unsaturated optically thick lines make the dominant contribution to the flow instability. Relaxation of assumptions (1), (2), and (6) is

discussed in §IV below. Subsequent papers in this series will examine relaxation of various remaining assumptions, particularly (12).

### *b) The Transfer Equation in the Co-Moving Frame*

We begin by considering the transfer equation in a co-moving frame representation for spherically-symmetric outflow (assumption [7]), in which we include the effects of sphericity in the frequency derivative, but not in the spatial gradient (See Rybicki 1970 for a discussion of this approximation.),

$$\mu \frac{\partial I}{\partial r} - Q \frac{\partial I}{\partial x} = -\chi \phi(x) \left[ I - S \right]. \tag{1}$$

Here

$$Q \equiv \frac{1}{v_{th}} \left[ \mu^2 v' + \left( 1 - \mu^2 \right) \frac{v}{r} \right], \tag{2}$$

$r$ is the radius, $\cos^{-1}\mu$ is the angle between the ray and the outward radial direction, $x$ is the frequency displacement from line center measured in the comoving frame in units of the Doppler width $\Delta\nu_D$, $v$ is the flow speed, $v' \equiv dv/dr$, $\phi(x)$ is the line profile function, $I$ is the specific intensity, and the line strength $\chi$ is related to the line opacity $\kappa$ through the mass density $\rho$ by $\chi = \rho\kappa$.

Under assumptions (1), (4), and (5) of pure, isotropic scattering with complete redistribution, the line source function $S$ is given by the mean line intensity,

$$S = \overline{J} = \left\langle \overline{I} \right\rangle, \tag{3}$$

where the bar denotes an average over the line profile

$$\overline{I}(r,\mu) \equiv \int_{-\infty}^{\infty} dx\, \phi(x) I(r,\mu,x), \tag{4}$$

and the angle brackets denote an average over angle,

$$\left\langle \overline{I} \right\rangle \equiv \tfrac{1}{2} \int_{-1}^{1} d\mu\, \overline{I}(r,\mu). \tag{5}$$

Finally, the line flux,

$$\overline{H} \equiv \left\langle \mu \overline{I} \right\rangle, \tag{6}$$

determines the line force per unit mass $g$ through

$$g = \left( \frac{4\pi\kappa\, \Delta\nu_D}{c} \right) \overline{H}. \tag{7}$$

### *i) The mean line force and scattered radiation field*

From the above we see that, to obtain the response of the line force to perturbations, we must obtain the perturbed line flux. Toward this goal, let us first divide the flow into a zero order mean state plus a first order sinusoidal perturbation,

$$v(r,t) = v_0(r) + v_1 e^{i(kr - \omega t)}, \tag{8}$$

with corresponding mean and perturbed values of other variables similarly denoted by "0" and "1" subscripts, respectively. The zero order transfer equation is then given by

$$Q_0 \frac{\partial I_0}{\partial x} = \chi_0 \phi(x) \left[ I_0 - S_0 \right], \tag{9}$$

where, in accordance with the Sobolev approximation (assumption [8]), all spatial derivatives of mean flow variables are ignored in favor of frequency derivative terms (Sobolev 1957, 1960), that is, $(\partial I_0/\partial r)_x = 0$. The Sobolev optical thickness in direction $\mu$ is defined by

$$\frac{1}{\tau_\mu} \equiv \frac{Q_0}{\chi_0} = \frac{1-\mu^2}{\tau_0} + \frac{\mu^2}{\tau_1}, \tag{10}$$

where[1] $\tau_0 \equiv \chi_0 r v_{th}/v_0$ and $\tau_1 \equiv \chi_0 v_{th}/v_0'$ are the Sobolev optical depths in the transverse and radial directions. Alternatively, defining (Castor 1974),

$$\sigma(r) \equiv \frac{d \ln v_0(r)}{d \ln r} - 1, \tag{11}$$

we may write

$$\tau_\mu = \frac{\tau_0}{1 + \sigma \mu^2}. \tag{12}$$

For an isolated line (assumption [2]; The effect of line overlap is treated in §IVc.), the intensity on the blue wing of the line is fixed by the intensity from the underlying stellar core,

$$I(r, \mu, x \to \infty) = I_c D(\mu, r), \tag{13}$$

where $I_c$ is a constant specifying the magnitude of the core intensity and $D(\mu, r)$ is a function specifying its angle dependence at radius $r$. Under assumption (6) of no limb darkening (cf. §IVa), $D(\mu)$ is unity for $\mu > \mu_*$ and zero for $\mu < \mu_*$, where

$$\mu_*(r) \equiv \sqrt{1 - \left(\frac{R_*}{r}\right)^2}, \tag{14}$$

and where $R_*$ is the radius of the photosphere.

Using the integrating factor $\exp(-\tau_\mu \Phi(x))$, where

$$\Phi(x) \equiv \int_x^\infty \phi(x')\, dx', \tag{15}$$

we may integrate (9) with the boundary condition (13) to obtain

$$I_0 = I_c D(\mu) e^{-\tau_\mu \Phi(x)} + S_0 \left(1 - e^{-\tau_\mu \Phi(x)}\right). \tag{16}$$

[1] An exception to our notational convention, the subscripts on $\tau_0$ and $\tau_1$ here refer to $\mu = 0$ and $\mu = 1$, and not to the mean and perturbed states.

The frequency averaged intensity in the mean flow is

$$\overline{I}_0 = I_c D(\mu) p(\mu) + S_0 \left(1 - p\left(\mu\right)\right), \tag{17}$$

where

$$p(\mu) \equiv \int_{-\infty}^{\infty} dx\, \phi(x) e^{-\tau_\mu \Phi(x)} = \frac{1 - e^{-\tau_\mu}}{\tau_\mu} \tag{18}$$

is the angle-dependent escape probability. The line flux in the mean flow is thus

$$\overline{H}_0 \equiv \left\langle \mu \overline{I}_0 \right\rangle = I_c \left\langle \mu D(\mu) p(\mu) \right\rangle, \tag{19}$$

where the terms proportional to $S_0$ have vanished because they are odd functions of $\mu$, with the result that the mean line force $g_0 \sim \overline{H}_0$ (see equation [7]) is independent of the scattered radiation field (Sobolev 1957, 1960; Lucy 1971; Castor 1974). Under assumption (3) of a strong line with $\tau_\mu \gg 1$, equation (19) becomes,

$$\overline{H}_0 = I_c \left\langle D \frac{\mu}{\tau_\mu} \right\rangle = I_c \left(\frac{R_*}{2r}\right)^2 \frac{1}{\tau_*} \tag{20}$$

where

$$\frac{1}{\tau_*} \equiv \frac{1 + \sigma\left(1 + \mu_*^2\right)/2}{\tau_0} = \frac{1}{2}\left(\frac{1}{\tau_1} + \frac{1}{\tau_{\mu_*}}\right). \tag{21}$$

Using equation (7), the mean line force is thus

$$g_0 = \pi I_c \left(\frac{R_*}{r}\right)^2 \frac{\kappa \Delta \nu_D}{c \tau_*}. \tag{22}$$

We now turn to the problem of solving for the mean scattered radiation field. From equation (3), the mean source function is

$$S_0 = \overline{J}_0 = I_c \frac{\beta_c}{\beta}, \tag{23}$$

where

$$\beta = \langle p(\mu) \rangle \tag{24}$$

is the angle-averaged escape probability and

$$\beta_c = \langle D(\mu) p(\mu) \rangle \tag{25}$$

is the core penetration probability. For the case of interest here of a strong line with $\tau_\mu \gg 1$, we find,

$$\frac{S_0}{I_c} = \frac{\beta_c}{\beta} = \left(\frac{1 - {\mu_*}^2}{2}\right)\left(\frac{1 + \sigma E_3}{1 + \sigma/3}\right), \tag{26}$$

where we have introduced the notation,

$$E_n \equiv \frac{1}{n}\frac{1-\mu_*{}^n}{1-\mu_*} = \frac{1}{n}\sum_{j=1}^{n}\mu_*{}^{j-1}. \tag{27}$$

Finally, we write the solution to the zero order transfer equation in the form,

$$I_0 - S_0 = I_c e^{-\tau_\mu \Phi(x)}\left[D - \frac{\beta_c}{\beta}\right]. \tag{28}$$

*ii) The perturbed line force and scattered radiation field*

Next we consider the problem of solving for the *perturbed* scattered radiation field. The first order transfer equation for the perturbed intensity $I_1$ is

$$ik\mu I_1 - Q_0\frac{\partial I_1}{\partial x} - Q_1\frac{\partial I_0}{\partial x} = -\chi_0\phi(x)\left[I_1 - S_1\right], \tag{29}$$

where we have used assumption (9) and the WKB approximation (cf. paper I) in ignoring a term proportional to $\chi_1$. In addition,

$$Q_1 = \frac{v_1}{v_{th}}\left[ik\mu^2 + \frac{1-\mu^2}{r}\right] \approx ik\mu^2\frac{v_1}{v_{th}}, \tag{30}$$

the latter approximation also being valid in the WKB limit $kr \gg 1$. Using equations (9), (10), and (28), we write equation (29) as,

$$-\frac{\partial I_1}{\partial x} + (\tau_\mu + i\mu K_\mu I_1) = \tau_\mu\phi(x)\left[S_1 + I_c e^{-\tau_\mu\Phi(x)}\left(D - \frac{\beta_c}{\beta}\right)\frac{Q_1}{Q_0}\right], \tag{31}$$

where we have defined

$$K_\mu \equiv \frac{k}{Q_0(\mu)}. \tag{32}$$

Then with the integrating factor $\exp(-i\mu K_\mu x + \tau_\mu\Phi(x))$ and the blue-wing boundary condition $I_1(r,\mu,x\to\infty) = 0$, equation (29) can be integrated to yield

$$I_1(r,\mu,x) = S_1\tau_\mu e^{i\mu K_\mu x - \tau_\mu\Phi(x)}\int_x^\infty dx'\phi(x')e^{-i\mu K_\mu x' + \tau_\mu\Phi(x')} +$$

$$+ I_c\tau_\mu\frac{Q_1}{Q_0}\left(D - \frac{\beta_c}{\beta}\right)e^{i\mu K_\mu x - \tau_\mu\Phi(x)}\int_x^\infty dx'\phi(x')e^{-i\mu K_\mu x'}. \tag{33}$$

Averaging over frequency then yields

$$\bar{I}_1(r,\mu) = S_1 A + I_c\left[D - \frac{\beta_c}{\beta}\right]\frac{Q_1}{Q_0}B, \tag{34}$$

where

$$A(\mu) \equiv \tau_\mu \int_{-\infty}^{\infty} dx\, \phi(x) e^{i\mu K_\mu x - \tau_\mu \Phi(x)} \int_x^{\infty} dx'\, \phi(x') e^{-i\mu K_\mu x' + \tau_\mu \Phi(x')} \tag{35}$$

and

$$B(\mu) \equiv \tau_\mu \int_{-\infty}^{\infty} dx\, \phi(x) e^{i\mu K_\mu x - \tau_\mu \Phi(x)} \int_x^{\infty} dx'\, \phi(x') e^{-i\mu K_\mu x'}. \tag{36}$$

The numerical evaluation of $A(\mu)$ and $B(\mu)$ is discussed in the Appendix.

Averaging equation (34) over angle, we obtain

$$\overline{J}_1 = S_1 \langle A \rangle + I_c \left\langle \left( D - \frac{\beta_c}{\beta} \right) \frac{Q_1 B}{Q_0} \right\rangle. \tag{37}$$

Then, since by equation (3), $S_1 = \overline{J}_1$, equation (37) may be solved for the perturbed source function,

$$S_1 = \frac{I_c}{1 - \langle A \rangle} \left\langle \left( D - \frac{\beta_c}{\beta} \right) \frac{Q_1 B}{Q_0} \right\rangle, \tag{38}$$

which may be used to eliminate $S_1$ from equation (34). Finally, taking the first angle moment of equation (34), we obtain the perturbed flux,

$$\overline{H}_1 = I_c \left\langle \left( D - \frac{\beta_c}{\beta} \right) \left( \mu + \frac{\langle \mu A \rangle}{1 - \langle A \rangle} \right) \frac{Q_1 B}{Q_0} \right\rangle. \tag{39}$$

Note from equation (35) that, since $\tau_\mu$ and $K_\mu$ are even functions of $\mu$, the real (imaginary) part of $A$ is an even (odd) function of $\mu$. Thus, $\langle A \rangle$ is purely real, while $\langle \mu A \rangle$ is purely imaginary, and the dependence of $\overline{H}_1$ on the perturbed scattered field can be written in terms of the real ratio,

$$\eta \equiv \frac{\langle \mu\, \Im A \rangle}{1 - \langle \Re A \rangle} = \frac{-i \langle \mu A \rangle}{1 - \langle A \rangle}. \tag{40}$$

Since $g \sim \overline{H}$, the perturbed line force $g_1$ can be written in terms of $\overline{H}_1$ and mean flow quantities,

$$\frac{g_1}{g_0} = \frac{\overline{H}_1}{\overline{H}_0}. \tag{41}$$

From equations (20), (30), (32) and (39), we then find

$$\begin{aligned} \frac{g_1}{v_1} &= \frac{g_0 \tau_*}{v_{th}} \left( \frac{2r}{R_*} \right)^2 \left( \frac{\overline{H}_1}{I_c} \frac{v_{th}}{v_1} \right) \\ &= \frac{g_0 \tau_*}{v_{th}} \left( \frac{2r}{R_*} \right)^2 \left\langle \left( D - \frac{\beta_c}{\beta} \right) (\mu + i\eta)\, i\mu^2 K_\mu B \right\rangle. \end{aligned} \tag{42}$$

The evaluation of the required angular averages is discussed in the Appendix. An approximation to $g_1/v_1$ can be obtained by using equation (A3), yielding

$$\frac{g_1}{v_1} \approx \omega_* \frac{k}{\chi_*} \left( \frac{2r}{R_*} \right)^2 \left\langle \left( D - \frac{\beta_c}{\beta} \right) \frac{\mu^2 \left[ \mu^2 K_\mu / (2x_*) - \eta \right] + i\mu^3 \left[ 1 + \eta K_\mu / (2x_*) \right]}{1 + \left[ \mu K_\mu / (2x_*) \right]^2} \right\rangle, \tag{43}$$

where $\omega_* = 2x_* g_0/v_{th}$ and $\lambda_* \equiv \chi_*^{-1} = \tau_*/(2x_*\chi_0)$ are generalizations of the growth rate and bridging length of paper I, now derived for the case that the stellar core has a finite angular size ( $\mu_* \neq 1$). As shown in paper I, the real parts of the perturbed force to velocity ratio, $\Re(g_1/v_1)$, essentially[2] gives the contribution of the line to the growth rate of flow perturbations; therefore, we shall henceforth refer to the ratio simply as the "line growth rate."

## III. RESULTS

To evaluate the perturbed force at a specific radius $r$ in the wind, we must assume a specific velocity law in order to determine terms which depend on $\sigma \equiv (d \ln v_0/d \ln r) - 1$. We may then use straightforward numerical angle quadrature to calculate from equation (43) the perturbed line force as a function of wavenumber $k$. For all detailed calculations presented here we assume a velocity law of the form

$$v_0(r) = v_\infty \left[1 - \left(\frac{R_*}{r}\right)\right]^p , \tag{44}$$

for which

$$\sigma(r) = \frac{(p+1)R_* - r}{r - R_*} . \tag{45}$$

For a velocity power index $p = \frac{1}{2}$, the outward acceleration of the wind is everywhere proportional to the local inward acceleration of gravity, in agreement with the theoretical result of CAK; however, observations appear to suggest (Abbott 1982) a less steep velocity law with $p \approx 1$–$2$. We shall show that any of these choices for $p$ yield qualitatively similar results for the wind instability.

### *a) Optically Thin Perturbations*

In the very short wavelength, optically thin perturbation case, $k \gg \chi$, we expect that the perturbed radiation field will be very small due to spatial averaging over the perturbed source function $S_1$. This is confirmed in the Appendix, where it is shown that $\eta \to 0$ in this limit. Using this fact and equation (A17), we see from equation (42) that the perturbed force becomes predominantly real and independent of scattered field perturbations. Using equations (20) and (41), we can express the perturbed force ratio in the form,

$$\begin{aligned} \frac{g_1}{v_1} \approx \Re\left(\frac{g_1}{v_1}\right) &= \omega_* \left\langle \left(D - \frac{\beta_c}{\beta}\right) \frac{\mu^2}{\tau_\mu} \right\rangle \Big/ \left\langle D \frac{\mu}{\tau_\mu} \right\rangle \\ &= \omega_* \frac{2}{1+\mu_*} \left[ \frac{(1+\sigma/3)(E_3 + \sigma E_5) - (1+\sigma E_3)(1/3 + \sigma/5)}{(1+\sigma/3)(1+\sigma(1+\mu_*^2)/2)} \right] \end{aligned} \tag{46}$$

with $E_3$ and $E_5$ defined in equation (27). The first term in the numerator results from the direct extinction of "core" radiation from the stellar photosphere, while the second term results from the drag effect of the mean scattered radiation field.

[2] I.e., exactly for the case of zero sound speed and within a factor of 2 otherwise.

Figure 1 shows the radial variation of $\Re(g_1/v_1)$ as calculated from equation (46) for the velocity laws given by equation (44) with $p = \frac{1}{2}$, 1 and 2. Comparison with the analogous curves for a pure absorption line shows how the scattering-line growth rate, as given by $\Re(g_1/v_1)$ (see paper I), is reduced by the drag effect of the mean scattered radiation field $S_0$. Near the base of the wind, the growth rate is essentially zero; but as the flow moves outward from the base, it rapidly increases, reaching 50% of the rate for pure absorption lines within a stellar radius from the base, and eventually approaching 80% of that rate far from the star. This still implies that perturbations in a wind driven by scattering lines will grow by many $e$-folds within a characteristic wind outflow time. We conclude that the bulk of such a wind is still very unstable to short wavelength, optically thin perturbations, even when the drag effect of the mean scattered radiation field is taken into account.

*b) Dependence on Perturbation Wavelength*

We now wish to establish the behavior of the perturbed force law $g_1/v_1$ as a function of wavenumber $k$, thus establishing the "bridging law" for the case of scattering lines.

As the first step, we evaluate by numerical quadrature the quantity $\eta$, defined in equation (40), using equations (A9) and (A10) of the Appendix. Results as a function of normalized wavenumber $k/\chi_*$ are given in figure 2 for a line with radial optical depth $\tau_1 = 100$ at various radii $r$ in a wind with a velocity law given by equation (44) (with $p = \frac{1}{2}$). Note that $\eta \to 0$ for both $k \ll \chi_*$ and $k \gg \chi_* \tau_1 \approx \chi$, in accord with our physical expectation that the effect of the perturbed scattered radiation field vanishes in both the Sobolev and optically-thin perturbation limits. (See also the discussion in the Appendix.) The perturbed field can therefore, at most, affect the instability of perturbations with a wavelength $\lambda$ smaller than the Sobolev length $L$ ($\approx 1/\chi_*$), but larger than a line-center mean-free-path $1/\chi$ ($\approx L/\tau_1$). Note also that $\eta < 0$ for all $k$. As we shall see, this means that the perturbed scattered field typically causes a slight increase in the strength of the instability, in contrast with the decrease caused by the mean scattered field.

Using numerical quadrature to evaluate the angle averages in equation (43), we may now calculate the variation of the perturbed force with wavenumber $k$. In figures 3a–3d we plot for a line with radial optical depth $\tau_1 = 100$ the results of such a calculation at selected radii, $r/R_* = 1.01$, 1.5, 2.5, and 10 in a wind with $p = \frac{1}{2}$. The perturbed force to velocity ratio $g_1/v_1$ is scaled here in units of $\omega_*$ while the wavenumber $k$ is scaled in units of $\chi_*$. For comparison, we also plot this perturbed force ratio in the absence of any scattered field (i.e., setting both $S_0 = S_1 = 0$), as well as in the absence of any perturbations in an existing mean scattered field (i.e., setting only $S_1 = 0$). In each case, the solid curves denote $\Re(g_1/v_1)$, and the dashed curves denote $\Im(g_1/v_1)$. Recall again (see paper I) that, while $\Re(g_1/v_1)$ essentially determines the growth rate of perturbations, $\Im(g_1/v_1)$ determines the speed of their phase propagation.

Concentrating first on the dashed curves in figure 3, note that the mean scat-

tered field $S_0$ has no effect at all on $\Im(g_1/v_1)$. This can be understood directly from equation (43), for which we note that the the imaginary part is odd in $\mu$, so that only the term representing the effect of direct radiation from the star contributes to $\Im(g_1/v_1)$. On the other hand, *perturbations* in the scattered field do have a dramatic effect on $\Im(g_1/v_1)$, reducing it to *negative* values for moderate and short wavelength perturbations ($\lambda \lesssim \lambda_* \approx L$). (Because of the logarithmic scale of the ordinate, we have actually plotted $|\Im(g_1/v_1)|$ in figure 3). As we shall see in the next section, this change in sign in $\Im(g_1/v_1)$ results in a like change in sign in the phase propagation of radiative-acoustic waves of moderate to short wavelength.

Concentrating next on the solid curves, note from figure 3a that including the *mean* scattered field $S_0$ substantially reduces the magnitude of $\Re(g_1/v_1)$ for short wavelength ($\lambda \ll \lambda_* \approx L$) perturbations near the base of the wind ($r = 1.01R_*$) (cf. curve with $S_0 = 0$ vs. those with $S_0 \neq 0$). As discussed above, this reduction results from the "photon drag" exerted on the velocity perturbations by the mean scattered field. Comparison with figures 3b–3d again shows that this drag effect quickly becomes less important as the gas moves away from the wind base ($r \gtrsim 1.5R_*$). In addition, note that including the *perturbed* scattered radiation field $S_1$ only slightly alters $\Re(g_1/v_1)$, generally increasing it somewhat for long wavelength ($\lambda \gtrsim \lambda_* \approx L$) perturbations near the star, but otherwise hardly changing it at all. Thus, insofar as the instability of the wind is concerned, we see that the overall effect of including scattering is to reduce the growth rate substantially very close to the star, but only slightly far from the star.

### *c) Linear Stability-Dispersion Analysis*

We now apply this calculation of the perturbed force associated with a scattering line to a linear stability-dispersion analysis in which we determine the growth and propagation characteristics of small-amplitude perturbations in a flow driven by line scattering. For a small-amplitude velocity perturbation $v_1$ with associated perturbed force $g_1$, the stability-dispersion equation relating the frequency $\omega$ to the wavenumber $k$ can be written (see paper I)

$$\omega^2 - i\frac{g_1}{v_1} - \gamma a^2 k^2 = 0, \tag{47}$$

where

$$\gamma \equiv 1 + \frac{2}{3}\frac{\omega}{\omega + iW} \tag{48}$$

describes the dependence of the perturbed pressure gradient force on the frequency $\omega$ and the temperature relaxation rate $W$. For the sake of brevity, we will only give details for the isothermal ($W \gg \omega$; $\gamma = 1$) and adiabatic ($W \ll \omega$; $\gamma = 5/3$) limits. (The results for the intermediate damping case, $\omega \approx W$, are quite similar to those of paper I.) Since the factor $\gamma$ in both these extremes is independent of frequency, we may use the quadratic formula to solve equation (47),

$$\omega_\pm = \frac{ig_1/v_1 \pm \sqrt{4\gamma a^2 k^2 - (g_1/v_1)^2}}{2}, \tag{49}$$

where $g_1/v_1$ is calculated from equation (43) using the velocity law (44).

In figures 4a and 4b, we plot the real (solid curves) and imaginary (dashed curves) parts of the two frequency modes $\omega_+$ and $\omega_-$ (scaled by $\omega_*$ ) vs. the wavenumber $k$ (scaled by $\chi_*$) for various values of the sound speed $\sqrt{\gamma}a$ (scaled by $\omega_*/\chi_*$) at the typical stellar wind radius $r = 2.5R_*$. The results are quite similar to those plotted in figure 3 of paper I. The major difference is found in $\Re(\omega_\pm)$, which changes sign for a wavenumber $k \approx 2\chi_*$. (Because of the logarithmic scaling of the ordinate, we have actually plotted $|\Re(\omega_\pm)|$). This indicates that short wavelength perturbations in a flow driven by scattering lines have their phase propagation in the opposite direction from those in the absorption line driven case studied in paper I. This effect has important consequences for how information about a perturbation propagates through the wind, a topic which we shall examine in more detail in a future paper of this series.

In contrast to this qualitative change in $\Re(\omega_\pm)$, note that the variation of the growth rate $\Im(\omega_\pm)$ with wavenumber $k$ is only slightly reduced relative to the pure absorption case. The major effect of scattering on the instability of the wind is thus to reduce the growth rate of short wavelength perturbations as a result of the drag effect of the mean scattered radiation field.

## IV. DISCUSSION OF OTHER EFFECTS

### *a) Effect of Limb Darkening*

We may easily generalize the above analysis of the perturbed line-scattering force to include the effects of limb darkening of the incoming stellar photospheric "core" radiation field. In this case, the angular dependence of the core intensity (cf. equation (13)) for $\mu > \mu_*$ is given by

$$D(\mu) = \frac{I(R_*, \nu)}{I(R_*, 1)}. \tag{50}$$

Here $I$ is the emergent continuum intensity from the stellar photosphere as a function of $\nu = \cos(\theta_*)$, where $\theta_*$ is the angle between the line of sight and the outward normal at the stellar surface. From elementary trigonometry, we may write $\nu$ as a function of $\mu$ as

$$\nu(\mu, r) = \left[\frac{\mu^2 - {\mu_*}^2}{1 - {\mu_*}^2}\right]^{\frac{1}{2}}. \tag{51}$$

With the minor modification of using equation (50) for $D(\mu)$, the analysis for the perturbed line force then proceeds as in §II.

In general, the limb darkening law depends on the continuum frequency relevant to the particular line under discussion. For purposes of illustration, let us choose a limb darkening law to be the same as for the frequency-integrated Eddington limb darkening law, so that

$$D(\mu) = \frac{3}{5}\left(\frac{2}{3} + \nu(\mu, r)\right), \tag{52}$$

(cf. Mihalas (1978), equation (3-37)). For this case, we find that the effect of limb darkening on the $\Im(g_1/v_1)$, and hence on the phase propagation of radiative-acoustic waves, is negligible. We further find that the effect on the $\Re(g_1/v_1)$, and hence on the instability growth rate, is also small, except that now $\Re(g_1/v_1) \approx 0.026\,\omega_* > 0$ at $r = R_*$, so that a wind driven by scattering lines is unstable, even at its base. If, on the other hand, the photospheric field were limb *brightened* (which is perhaps unlikely), then flow perturbations at the base of such a wind would be mildly *damped.*

It is interesting to note in this regard that, in the coherent scattering analysis of Lucy (1984), the cancellation of the instability is specific only to the assumption that the flow is plane parallel, and is wholly *independent* of any assumption about the angular dependence of the incoming radiation in the blue wing of the line. Here we see that, under the physically more realistic assumption of scattering with complete redistribution, the relative importance of the drag effect depends critically on the angular dependence of the stellar photospheric radiation field, with exact cancellation of the instability occurring at the base of the wind when there is no limb darkening. Because of this sensitivity of the cancellation to assumptions about the line frequency redistribution and the angle dependence of the radiation field, a reliable answer to the question of whether the wind base is, in fact, unstable may require a more sophisticated treatment involving full angle- and frequency-dependent redistribution functions for the line scattering. This topic is currently under investigation.

### *b) Effect of Photon Destruction*

We may also readily generalize the analysis of §II to include the effects of photon destruction. (For simplicity, we still ignore the effect of any thermal creation of photons.) If the probability of destruction per scattering of the line photon is $\epsilon$, then the line source function relation, equation (3), becomes,

$$S = (1 - \epsilon)\overline{J}. \tag{53}$$

We may therefore still use equation (43) for the perturbed force if we just modify the definition of terms that arise from the mean and perturbed scattered field. We accomplish this by changing the definition of the core penetration probability (cf. equation (25))

$$\beta_c = (1 - \epsilon)\,\langle D(\mu)\beta(\mu)\rangle\,, \tag{54}$$

and the perturbed scattered field ratio (cf. equation (40)),

$$\eta = (1 - \epsilon)\frac{\langle \mu\, \Im A\rangle}{\langle 1 - \Re A\rangle}. \tag{55}$$

Note then that for $\epsilon = 1$, we obtain $\beta_c = \eta = 0$ and thereby recover the pure absorption results (cf. curves labeled $S_0 = S_1 = 0$ in figure 3). In general, the results for the case of $0 < \epsilon < 1$ are intermediate between those for the $\epsilon = 0$ and $\epsilon = 1$ cases as plotted in figure 3.

### *c) Effect of Line Overlap*

Many of the lines which drive stellar winds are not effectively isolated from neighboring lines (Abbott 1980, 1982; Olsen 1982; Friend and Castor 1983; Abbott and Lucy 1985), as we assumed in §II (assumption 2); instead they often "overlap" within the wind because their rest wavelengths $\lambda_0$ are separated by less than the maximum Doppler shift, $2\lambda_0 v_\infty/c$, between two points in the wind. In justifying his contention that line-driven stellar winds are not as unstable as previously thought, Lucy (1984) has asserted that in the outer parts of winds, line drag results in a damping contribution from resonance lines that are strongly shadowed by neighboring resonance transitions. We can examine this assertion quantitatively by generalizing the perturbation analysis of §II to the case of a pair of optically thick overlapping lines with a wavelength separation in velocity units of $\Delta v$, where $0 < \Delta v < 2v_\infty$. (Further generalization to sets of three or more overlapping lines is straightforward, but tedious.)

We first note that the above analysis for an isolated single line can be applied without modification to the bluer line of the pair. This is because radiation scattered in the wind always appears red-shifted when viewed from another location in the wind, and so scattering by the red line can have no effect on the blue line. On the other hand, for the red line we must generalize the single-line analysis to include the new possibility that radiation scattered by the blue line is subsequently redshifted into resonance with the red line. In this case, the boundary condition for the intensity on the blue wing of the red line is now (cf. equation [13]) given by the intensity scattered out of the red wing of the blue line. Letting $\mathbf{R} = \mathbf{R}(r, \mu, \Delta v)$ denote the blue line resonance point corresponding to the red line resonance point $\mathbf{r}$, the boundary condition can be written

$$I_r(r, \mu, x \to \infty) = I_b(R, \mu', x \to -\infty). \tag{56}$$

Defining $\mathbf{l} \equiv \mathbf{r} - \mathbf{R}$, we then have $\mu = \hat{\mathbf{l}} \cdot \hat{\mathbf{r}}$ and $\mu' = \hat{\mathbf{l}} \cdot \hat{\mathbf{R}}$, where a circumflex denotes the corresponding unit vector. The resonance condition between the two points is that the line separation $\Delta v$ is equal to the relative line-of-sight velocity along the ray,

$$\Delta v = [\mathbf{v}(\mathbf{r}) - \mathbf{v}(\mathbf{R})] \cdot \hat{\mathbf{l}}, \tag{57}$$

which, for radial outflow, becomes

$$\Delta v = \mu v(r) - \mu' v(R). \tag{58}$$

The resonance point radius $R = R(r, \mu, \Delta v)$ may be found as the solution of equation (58), eliminating $\mu'$ through the law of sines, $R^2(1 - \mu'^2) = r^2(1 - \mu^2)$.

We shall consider only the particular case of the velocity law (44) with $p = \frac{1}{2}$. In this case we find that $R$ is a root of the cubic,

$$\left[1 - \left(\frac{\Delta v - \mu v}{v_\infty}\right)^2\right] R^3 - R_* R^2 + \left(1 - \mu^2\right) r^2 \left(R_* - R\right) = 0. \tag{59}$$

In solving this equation, we seek real roots such that $R \geq R_*$. For fixed $r$ and $\Delta v$, there are no such roots when $-1 \leq \mu < \mu_{min}$, where

$$\mu_{min} \equiv \frac{\Delta v - v_\infty}{v(r)}. \tag{60}$$

For all other $\mu$, there is exactly one such root, but for $\mu_* < \mu < \mu_{max}$, where

$$\mu_{max} \equiv \frac{\Delta v}{v(r)}, \tag{61}$$

this root is associated with a resonance point that is obscured by the stellar core. When an unobscured resonance point does exist, then the intensity in the blue wing of the red line is given by equation (56); otherwise it is given by equation (13).

The distance $l$ that radiation travels between scatterings in the blue and red line can, in general, be on the order of a stellar radius or more. Since, in the local stability analysis conducted here, we are not concerned with effects that require perturbations to be coherent over such large distances, we ignore any effect that perturbations in the blue-line intensity might have on the red line. We therefore retain from §II the blue wing boundary condition $I_{1r}(r, \mu, x \to \infty) = 0$ for the *perturbed* red-line intensity. We do, however, modify the *mean* intensity to reflect these multiple scattering effects.

For the particular case that the blue line is optically thick (assumption 3), we find from equations (16) and (23) that

$$I_{0b}(R, \mu', x \to -\infty) = S_{0b}(R) = I_c \frac{\beta_{cb}(R)}{\beta_b(R)}. \tag{62}$$

where $\beta_b$ and $\beta_{cb}$ are evaluated by equations (24) and (25) for the blue line. Note that, although at *fixed* $R$, $S_{0b}$ is not a function of $\mu'$, in general we have $R = R(r, \mu, \Delta v)$, and so $S_{0b} = S_{0b}(R(\mu))$. Using equations (56) and (62), we may then generalize the function $D(\mu, r)$ (cf. equation (13)) to describe the overall angle dependence of the intensity in the blue wing of the red line,

$$D_r(\mu, r) = \begin{cases} 0, & -1 < \mu < \mu_{min} \\ \beta_{cb}(R)/\beta_b(R), & \mu_{min} < \mu < \mu_* \\ 1, & \mu_* < \mu < \mu_{max} \\ \beta_{cb}(R)/\beta_b(R), & \mu_{max} < \mu < 1. \end{cases} \tag{63}$$

The second equality represents the effect of backscattering by the blue line, whereas the last equality represents the effect of shadowing and subsequent forward scattering of the stellar core radiation. With these two blue-line scattering effects thus incorporated into the definition of $D$, the remainder of the perturbation analysis then proceeds as in §II. We thereby find that the red-line perturbed force $g_{1r}$ is also given by equation (43) if we just replace $D$ by $D_r$ and $\beta_c$ by $\beta_{cr} \equiv \langle D_r(\mu) p(\mu) \rangle$ (cf. equation (25)). These two modifications represent generalizations of the "direct"

and "drag" terms of the single-line perturbed force to include the additional effects of scattering by the overlapping blue line.

As we are primarily interested here in the effects of line overlap on the instability to optically thin perturbations, we restrict our discussion to results for the perturbation growth rate $\Re(g_1/v_1)$ in the short wavelength limit $k \gg \chi$. For a wind with the velocity law given by equation (44) with $p = \frac{1}{2}$, figs. 4a and 4b show the radial variation of the red-line growth rate $\Re(g_{1r}/v_1)$ for line pairs with velocity-unit wavelength separations $\Delta v$ ranging from $0.1v_\infty$ to $2v_\infty$. For the case of maximum separation $\Delta v = 2v_\infty$, the lines no longer overlap, and so we recover in this case the earlier result (cf. figure 1) for an isolated single line. Furthermore, since the blue line of a pair is never influenced by the red line, this isolated line result also gives the perturbed blue-line growth rate $\Re(g_{1b}/v_1)$.

For velocity separations in the range $v_\infty < \Delta v < 2v_\infty$ (figure 5b), note that the red-line growth rate actually *increases* with increasing line overlap. This is because, in this separation range, the dominant effect of line overlap is to enhance the "direct" term in equation (43) through backscattering by the blue line of radiation from the opposite side of the stellar wind. For $\Delta v < v_\infty$ (figure 5a), on the other hand, this direct term is diminished beyond the radius at which shadowing by the blue line reduces the intensity from the stellar core; the red-line growth rate at large radii thus now decreases with increasing overlap. For strongly overlapped lines ($\Delta v \lesssim 0.2v_\infty$), the combined effects of reduction in the direct term by shadowing and enhancement in the drag term by backscattering causes the net red-line growth rate to become slightly *negative* very near ($r \lesssim 1.1R_*$) the stellar surface. Since the growth rates for unshadowed lines all become very small near the surface, this result implies that the combined effect of an ensemble of overlapping lines would tend to make the very base of the stellar wind *stable*. (See however the discussion at the end of §IVa.) However, only slightly away from the surface ($r \gtrsim 1.1R_*$), the growth rates for even the strongly shadowed lines (e.g., $\Delta v = 0.1v_\infty$) again become positive, although they are still reduced relative to the growth rates for unshadowed lines. Since the growth rates for these unshadowed lines are all very large away from the wind base, the combined effects of an ensemble of shadowed and unshadowed lines is to make the bulk of the wind very unstable.

We may thus summarize the results of our analysis of line overlap by stating that, while the contribution of strongly shadowed lines to the flow instability (as well as to the flow driving) is indeed reduced compared to unshadowed lines, their overall effect in the outer parts of the wind is *not*, as claimed by Lucy (1984), one of damping. Since the unshadowed lines (e.g., the bluest line of a multiplet) still make a strong contribution to the growth rate, we can conclude again that such radiatively driven flows are very unstable.

## V. SUMMARY AND CONCLUSIONS

In this paper, we have extended our earlier study (paper I) of the stability of

line-driven stellar winds to take proper account of the finite angular size of the stellar photosphere and to include the dynamical effects of scattered radiation. Our work differs from the previous study of scattering by Lucy (1984) in that it is based on the physically more reasonable assumptions that the scattering occurs with complete redistribution (CRD) (vs. complete coherence) and that the mean wind flow is spherically symmetric (vs. plane parallel). Our results are summarized as follows:

1) The mean scattered radiation exerts a drag force on velocity perturbations, which can eliminate the contribution of scattering lines to the instability of the flow (Lucy 1984), but only at the base of the wind, and only if one ignores photospheric limb darkening. With limb darkening, the scattering-line growth rate at the wind base is positive, and is a few percent of the rate for pure absorption lines (derived in paper I).

2) As the flow moves outward from the base, the scattering-line growth rate rapidly increases to more than 50% of the rate for pure absorption lines within a stellar radius of the stellar surface, and eventually reaches 80% of that rate far from the star.

3) Perturbations in the scattered radiation field change the details of the "bridging law", which describes the response to intermediate wavelength perturbations, but this change is such as to affect mostly the propagation, and not the growth, of perturbations.

4) The contribution of the red component of an overlapping line pair to the wind instability may be reduced compared to that of isolated lines, but the overall effect is not one of damping in the bulk of the wind.

The basic conclusion we draw from these results is that the bulk of material in a radiatively driven stellar wind is still very unstable, even after all the effects of scattered radiation (including photon drag and line overlap) are taken into account.

It is a pleasure to acknowledge helpful discussions with D. Friend and K. MacGregor. This work was supported by the NASA HEAO-2 Guest Investigator Program and by NASA grant NSG-7406.

## APPENDIX: $A(\mu)$, $B(\mu)$ AND ASSOCIATED AVERAGES

In order to evaluate the various angular averages occuring in equations (37) through (40), we must be able to evaluate the quantities $A(\mu)$ and $B(\mu)$, defined in equations (35) and (36). We first note that the double integral defining $B(\mu)$ is identical to that in the expression for $\delta g/\delta v$ in paper I (equation [I-24]). In paper I a good approximation for $\delta g/\delta v$ was presented in equation (I-28), implying the

corresponding approximation

$$B(\mu) \approx \frac{1}{\tau_\mu + i\mu K_\mu/\phi(x_\mu)}. \qquad (A1)$$

Here the blue-edge absorption frequency $x_\mu$ is a slowly-varying function of $\tau_\mu$, given as the solution to the equation

$$\tau_\mu \Phi(x_\mu) = 1. \qquad (A2)$$

In the case of a Doppler profile for $\tau_\mu \gg 1$, $\phi(x_\mu) \approx 2x_\mu/\tau_\mu$, leading to the approximation

$$B(\mu) \approx \frac{1}{\tau_\mu [1 + i\mu K_\mu/(2x_*)]}. \qquad (A3)$$

Although $x_\mu$ is a function of $\mu$, we ignore this weak dependence in equation (A3) and take $x_\mu \approx x_* =$ constant in evaluating the angular averages.

We do not have a similar approximate expression for $A(\mu)$, so we must find other methods to evaluate it. Other methods are also necessary if it is desired to obtain more accurate values of $B(\mu)$ than those given by equation (A1). A convenient way to evaluate both $A(\mu)$ and $B(\mu)$, as well as their angular averages, is to express them in terms of Fourier integrals.

Let us define $\gamma_\mu = 1/\tau_\mu = \mu^2\gamma_1 + (1-\mu^2)\gamma_0$, in terms of which $K_\mu = K/\gamma_\mu$, where $K \equiv k/\chi_0$ is the wavenumber normalized by the mean line opacity $\chi_0$. By changing the variable of integration to $t = (x' - x)/\gamma_\mu$ in the inner integrals in equations (35) and (36), and interchanging the orders of integration, we obtain

$$A(\mu) = \int_0^\infty dt\, e^{-iK\mu t} K(t, \gamma_\mu), \qquad (A4)$$

$$B(\mu) = \int_0^\infty dt\, e^{-iK\mu t} \mathcal{L}(t, \gamma_\mu), \qquad (A5)$$

where

$$K(t,\gamma) = \int_{-\infty}^\infty dx\, \phi(x)\phi(x+\gamma t) \exp\left\{-\gamma^{-1}\left|\Phi(x) - \Phi(x+\gamma t)\right|\right\}. \qquad (A6)$$

$$\mathcal{L}(t,\gamma) = \int_{-\infty}^\infty dx\, \phi(x)\phi(x+\gamma t) \exp\left\{-\gamma^{-1}\Phi(x)\right\}. \qquad (A7)$$

The various angular averages of $A(\mu)$ and $B(\mu)$ can now easily be expressed as Fourier-type integrals. For example,

$$\langle A(\mu)\rangle = \tfrac{1}{2}\int_{-1}^1 d\mu\, A(\mu) = \tfrac{1}{2}\int_0^1 [A(\mu) + A(-\mu)]. \qquad (A8)$$

Since $\gamma_\mu$ is even in $\mu$, we have from equation (A4),

$$\begin{aligned}\langle A\rangle &= \int_0^1 d\mu \int_0^\infty dt\, \cos K\mu t\, K(t,\gamma_\mu) \\ &= \int_0^\infty dt\, \cos Kt \int_0^1 \frac{d\mu}{\mu} K(\frac{t}{\mu}, \gamma_\mu), \end{aligned} \qquad (A9)$$

using the transformation $t \to t/\mu$ and interchanging the order of integration. Similarly,

$$\langle \mu A \rangle = -i \int_0^\infty dt \sin Kt \int_0^1 d\mu \, K(\frac{t}{\mu}, \gamma_\mu). \qquad (A10)$$

From the values of $\langle A \rangle$ and $\langle \mu A \rangle$ the quantity $\eta$, defined in equation (40), can be found.

The required averages of $B$ are somewhat more complicated, since each involves both even and odd functions of $\mu$. These averages are most simply obtained using the approximations (A1) or (A3), but they can also be expressed in terms of Fourier-type integrals in a manner analogous to the derivation of equations (A9) and (A10). We omit the details but give the results:

$$\left\langle \left( D - \frac{\beta_c}{\beta} \right) \frac{ik\mu^2}{Q_0} B(\mu) \right\rangle = iK \int_0^\infty dt \, e^{-iKt\frac{1}{2}} \int_{\mu_*}^1 d\mu \, \frac{\mu}{\gamma_\mu} D(\mu) \mathcal{L}(\frac{t}{\mu}, \gamma_\mu)$$
$$- iK \int_0^\infty dt \cos Kt \, \frac{\beta_c}{\beta} \int_0^1 d\mu \, \frac{\mu}{\gamma_\mu} \mathcal{L}(\frac{t}{\mu}, \gamma_\mu), \quad (A11)$$

$$\left\langle \left( D - \frac{\beta_c}{\beta} \right) \mu \frac{ik\mu^2}{Q_0} B(\mu) \right\rangle = iK \int_0^\infty dt \, e^{-iKt\frac{1}{2}} \int_{\mu_*}^1 d\mu \, \frac{\mu^2}{\gamma_\mu} D(\mu) \mathcal{L}(\frac{t}{\mu}, \gamma_\mu)$$
$$- K \int_0^\infty dt \sin Kt \, \frac{\beta_c}{\beta} \int_0^1 d\mu \, \frac{\mu^2}{\gamma_\mu} \mathcal{L}(\frac{t}{\mu}, \gamma_\mu), \quad (A12)$$

The representation of these angular averages by means of Fourier integrals has several advantages: 1) The existence of standard numerical methods for evaluating Fourier integrals allows closer control of the cancellation of rapidly varying complex exponential or trigonometric terms, so that high accuracy can be obtained. 2) Since the wavenumber $K$ appears only in the final Fourier transform, the numerical work of evaluating the two inner integrals is much reduced. 3) Complex arithmetic, if required at all, comes in only during the last step of evaluating the Fourier integrals. 4) The asymptotic behavior at small and large wavenumbers can be found from well-known general results on Fourier integrals.

Let us now find the asymptotic behavior of $A$ and $B$ for large and small values of $K$, using the representations (A4) and (A5). For $K \to 0$ (Sobolev limit) we find

$$A \to \int_0^\infty dt \, K(t, \gamma_\mu) = 1 - p(\mu), \qquad (A13)$$

where $p(\mu)$ is defined in equation (18). In obtaining equation (A13) we have used equation (A6) and the fact that $d\Phi(x) = -\phi(x)\, dx$. Similarly for $K \to 0$ we find,

$$B \to p(\mu) - e^{-\tau_\mu}. \qquad (A14)$$

In this limit $A$ is purely real, so the imaginary part of $\langle \mu A \rangle$ vanishes. Thus $\eta \to 0$, implying that the perturbed scattered intensity field vanishes in the Sobolev limit, as was expected on the basis of simple arguments.

For $K \to \infty$ (optically thin perturbation limit), equations (A4) and (A5) yield the results $A \to 0$ and $B \to 0$, using the Riemann-Lebesgue lemma. This implies $\eta \to 0$, so that the perturbed scattered intensity field also vanishes in this limit. However, in the angular averages of equation (42), $B$ appears in the combination $i\mu K_\mu B$, which requires a more accurate estimation. We therefore integrate equation (A5) by parts once to obtain

$$i\mu K B = \mathcal{L}(0,\gamma_\mu) - \int_0^\infty dt\, e^{-iK\mu t} \frac{\partial}{\partial t} \mathcal{L}(t,\gamma_\mu). \qquad (A15)$$

Applying the Riemann-Lebesgue lemma for $K \to \infty$ and using $K_\mu = K\tau_\mu$, we find

$$i\mu K_\mu B \to \tau_\mu \mathcal{L}(0,\gamma_\mu). \qquad (A16)$$

We may also use the approximate equation (A3) to express this limit as

$$i\mu K_\mu B \to \frac{2x_*}{\tau_\mu}. \qquad (A17)$$

## REFERENCES


Abbott, D. C. 1980, *Ap. J.*, **242**, 1183.

Abbott, D. C. 1982, *Ap. J.*, **259**, 282.

Abbott, D. C. and Lucy, L.B. 1985, preprint.

Carlberg, R. G. 1980, *Ap. J.*, **241**, 1131.

Cassinelli, J. P. 1979, *Ann. Rev. Astron. Astrophys.*, **17**, 275.

Cassinelli, J. P. and MacGregor, K. B. 1985, in *Physics of the Sun*, ed. P. A. Sturrock, D. Mihalas, T. Holzer, and R. Ulrich (Holland: Dordrecht), in press.

Castor, J. I. 1970, *M. N. R. A. S.*, **149**, 111.

Castor, J. I. 1974, *M. N. R. A. S.*, **169**, 279.

Castor, J. I. Abbott, D. C. and Klein, R. I. 1975, *Ap. J.*, **195**, 157. (CAK).

Friend, D. B. and Castor, J. I. 1983, *Ap. J.*, **272**, 259.

Lucy, L. B. 1971, *Ap. J.*, **163**, 95.

Lucy, L. B. 1984, *Ap. J.*, **284**, 351.

Lucy, L. B. and Solomon, P. M. 1970, *Ap. J.*, **159**, 879.

MacGregor, K. B., Hartmann, L., and Raymond, J. C. 1979 (MHR), *Ap. J.*, **231**, 514.

Mihalas, D. 1978, *Stellar Atmospheres*, 2nd ed.; (San Francisco: Freeman).

Milne, E. A. 1926, *M. N. R. A. S.*, **86**, 459.

Olson, G. L. 1982, *Ap. J.*, **255**, 267.

Owocki, S. P. and Rybicki, G. B. 1984, *Ap. J.*, **284**, 337. (Paper I).

Rybicki, G. B. 1970, in *Spectrum Formation in Stars with Steady-State Extended Atmospheres*, ed. H. G. Groth and P. Wellmann, NBS Spec. Publ. 332, (Washington: U.S. Government Printing Office), p. 87.

Sobolev, V. V. 1957, *Soviet Astr. - A. J.*, **1**, 678.

Sobolev, V. V. 1960, *Moving Envelopes of Stars*, (Cambridge: Harvard Univ. Press).

## FIGURE CAPTIONS

Figure 1: Radial variation of the line growth rate (in units of the growth rate $\omega_*$ defined in text) for short wavelength, optically thin perturbations ($k \gg \chi$), as given by the perturbed line force to velocity ratio $g_1/v_1$. The upper (lower) curves are for a pure absorption (scattering) line, and the index $p$ measures the steepness of the assumed velocity law.

Figure 2: Wavenumber variation of the peturbed scattering ratio $\eta$ (defined by equation (40) in the text) for a line with radial optical depth $\tau_1 = 100$ at various radii $r$ in a wind with a velocity law given by equation (44) with $p = \frac{1}{2}$.

Figure 3: Wavenumber variation of real (solid curves) and imaginary parts of perturbed force to velocity ratio for a scattering line with radial optical depth $\tau_1 = 100$ at various radii $r/R_*$ in the wind. Curves labeled $S_0 = S_1 = 0$ denote results for pure extinction (no scattering) case, while curves labeled $S_1 = 0$ denote results if perturbations in an existing scattered field are ignored.

Figure 4: Stability-dispersion curves showing the wavenumber variation of the real (solid) and imaginary (dashed) parts of the frequency $\omega_\pm$ for outward (+) and inward (−) propagating radiative acoustic waves with various values of the sound speed $\sqrt{\gamma}a$.

Figure 5: Same as figure 1, except for the red component of an overlapping pair of scattering lines for various values of the velocity separation $\Delta v$.

## ADDRESSES OF AUTHORS

Stanley P. Owocki: UCSD/CASS, Mail Code C-011, La Jolla, CA 92093

George B. Rybicki: Harvard-Smithsonian Center for astrophysics, 60 Garden St., Cambridge, MA 02138

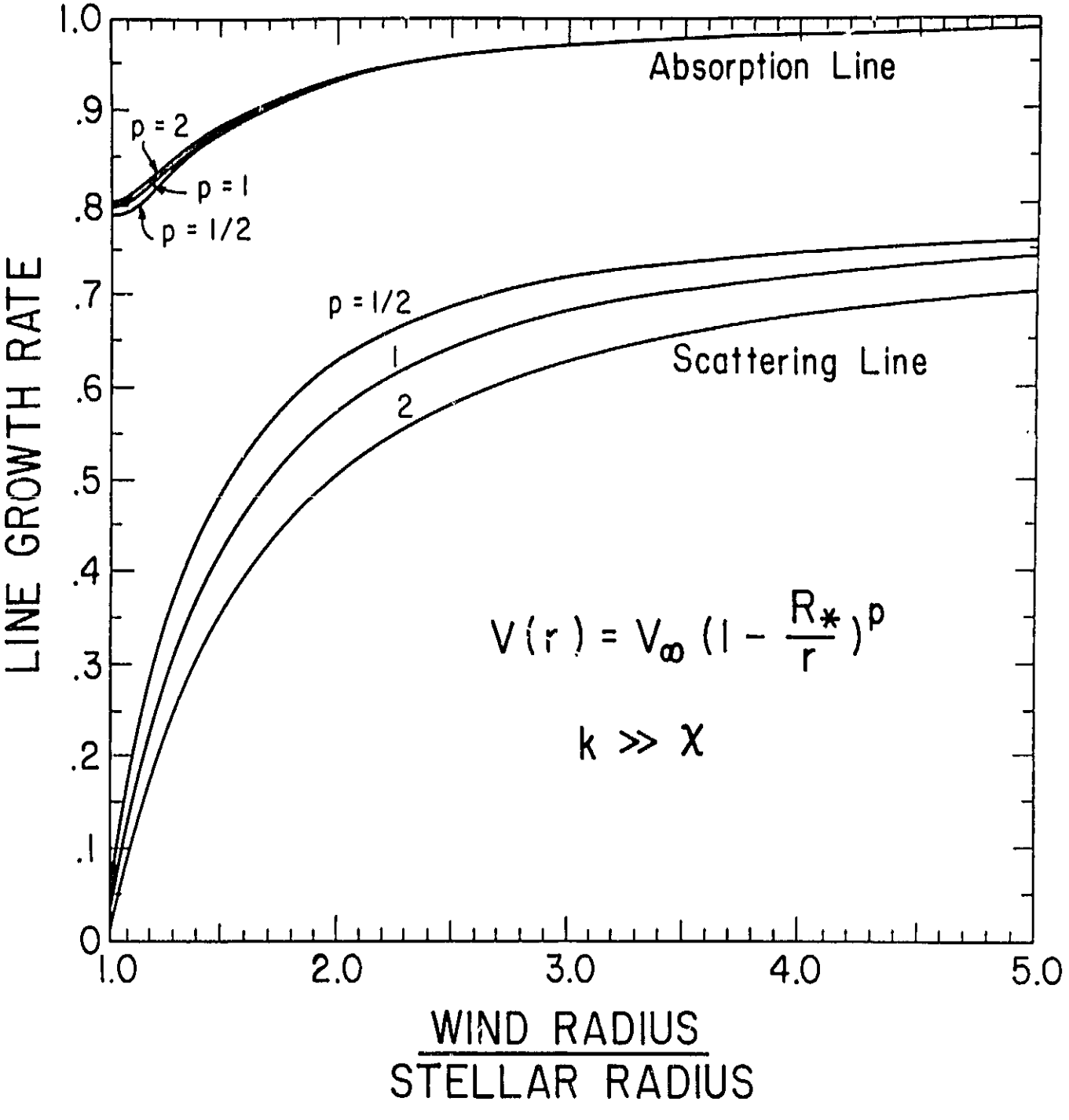
LINE GROWTH RATE
1.0
.9
.8
.7
.6
.5
.4
.3
.2
.1
0
Absorption Line
p = 2
p = 1
p = 1/2
p = 1/2
1
2
Scattering Line
$V(r) = V_\infty (1 - \frac{R_*}{r})^p$
$k \gg \chi$
1.0
2.0
3.0
4.0
5.0
WIND RADIUS
STELLAR RADIUS

Figure 1

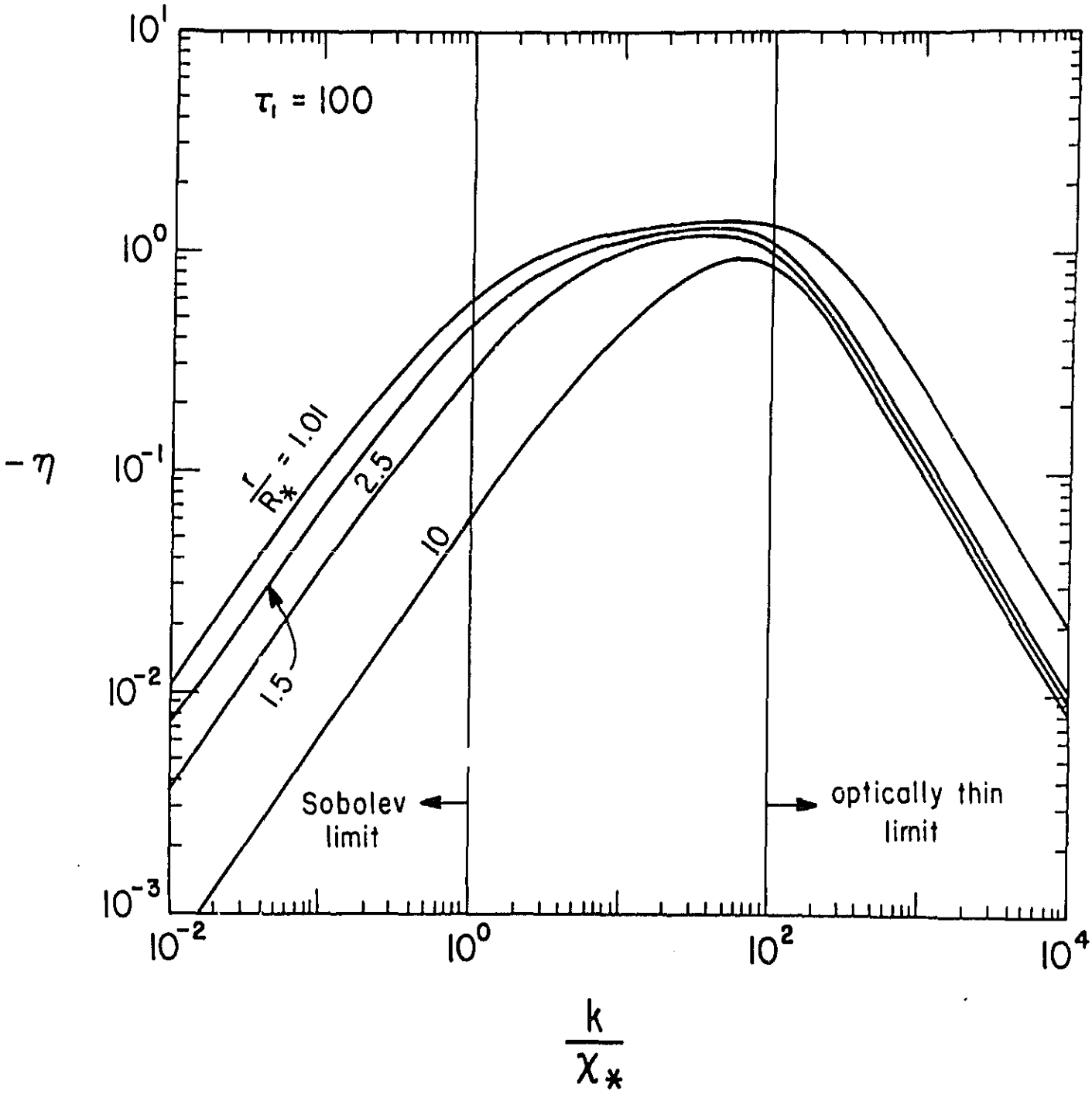
$\tau_1 = 100$
$\frac{r}{R_*} = 1.01$
2.5
1.5
10
Sobolev limit
optically thin limit
$-\eta$
$\frac{k}{\chi_*}$
$10^1$
$10^0$
$10^{-1}$
$10^{-2}$
$10^{-3}$
$10^{-2}$
$10^0$
$10^2$
$10^4$

Figure 2

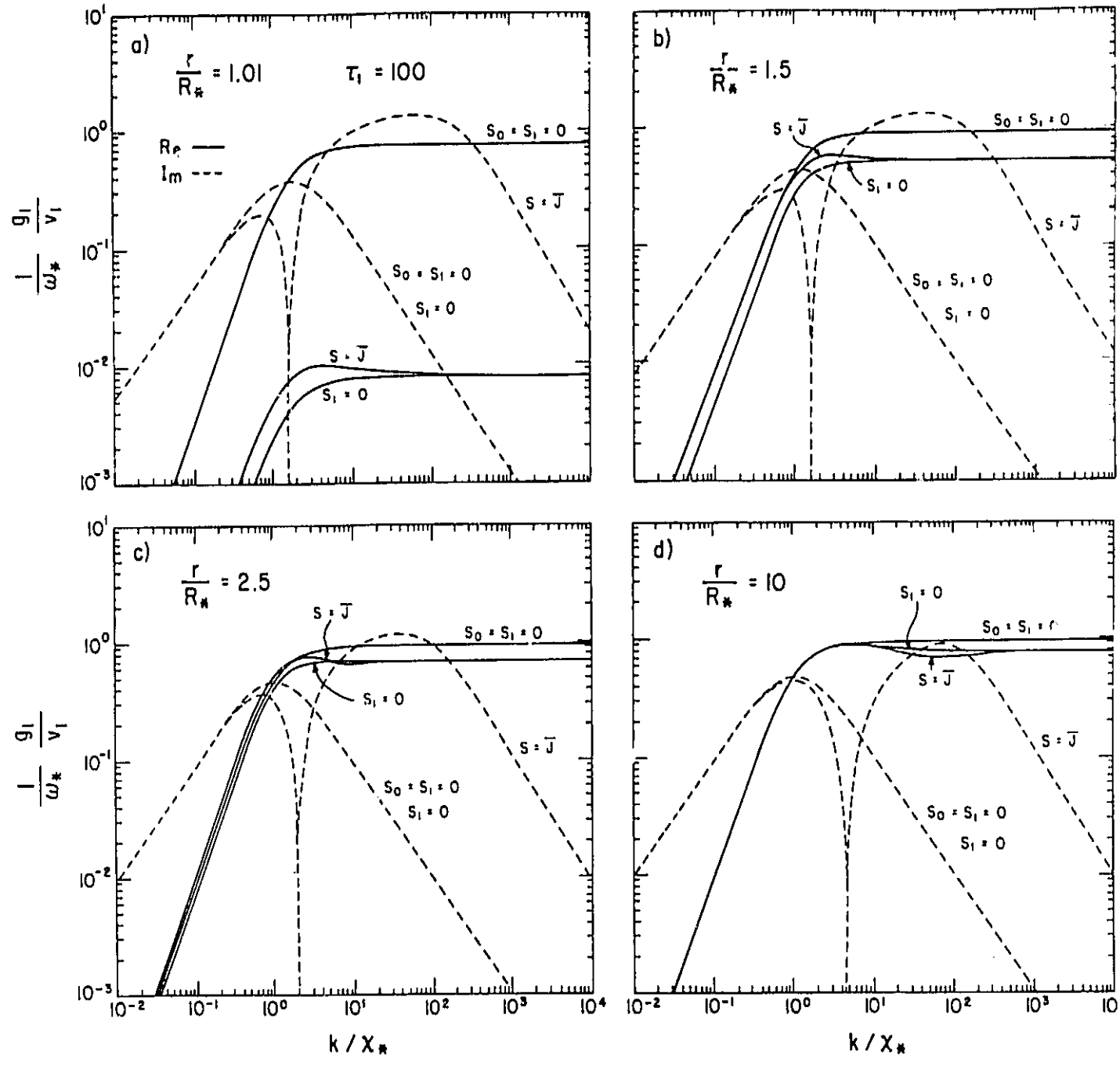


Figure 3

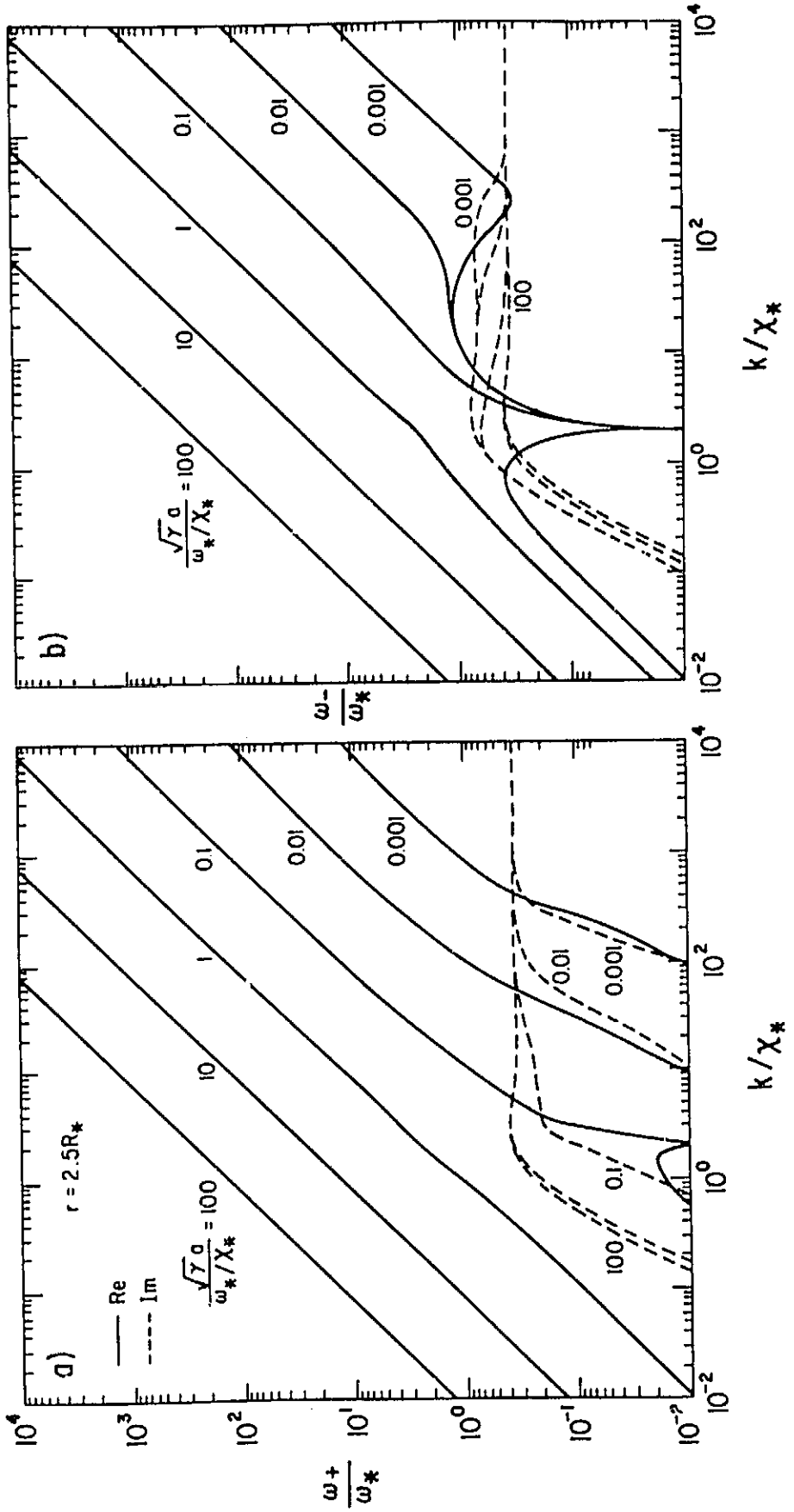
a)
r = 2.5R*
Re
Im
$\frac{\sqrt{\gamma}\,a}{\omega_*/\chi_*} = 100$
10
1
0.1
0.01
0.001
0.01
0.001
0.1
100
$\frac{\omega_+}{\omega_*}$
$k/\chi_*$
b)
$\frac{\sqrt{\gamma}\,a}{\omega_*/\chi_*} = 100$
10
1
0.1
0.01
0.001
0.001
100
$\frac{\omega_-}{\omega_*}$
$k/\chi_*$

Figure 4

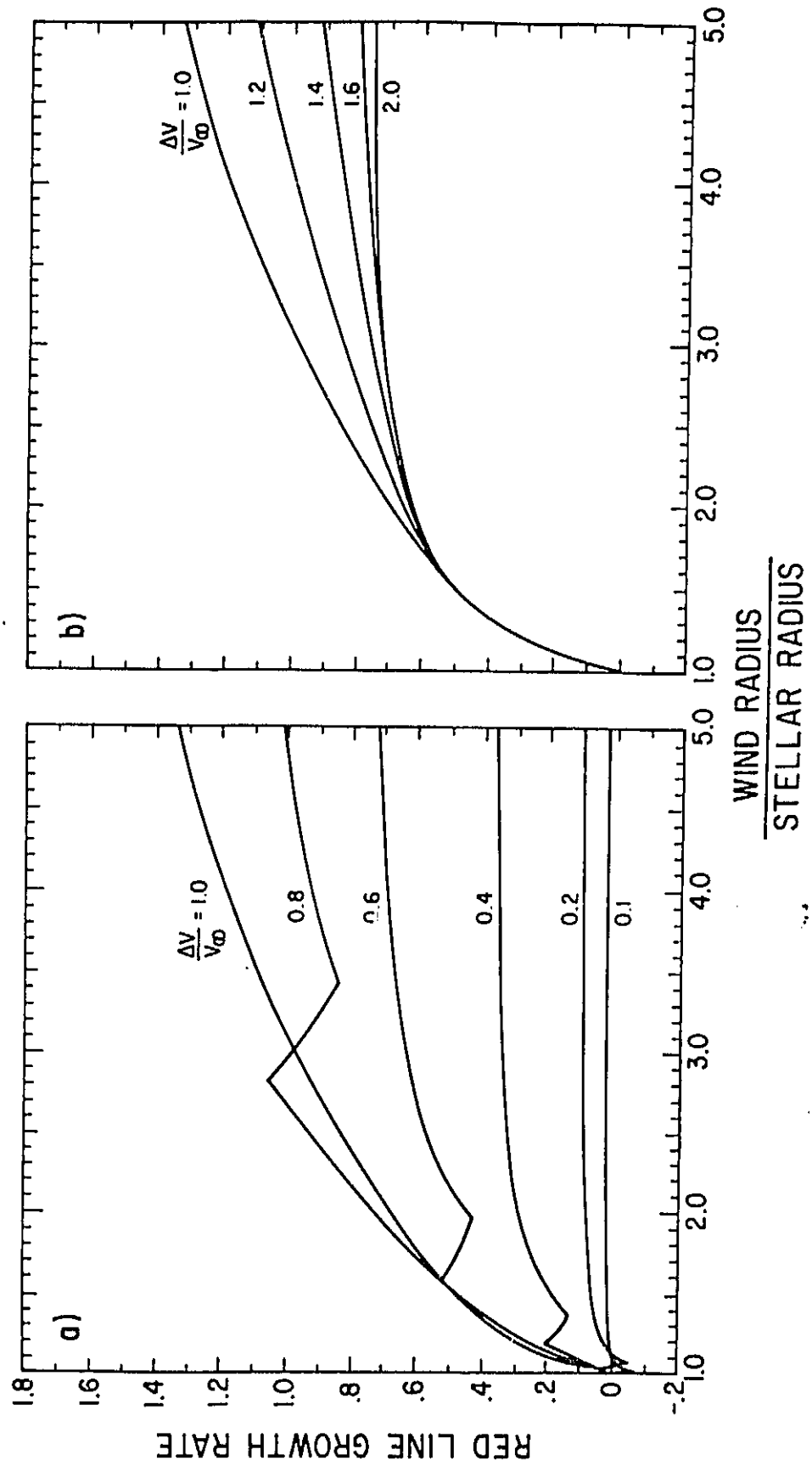
a)
b)
$\frac{\Delta V}{V_\infty} = 1.0$
0.8
0.6
0.4
0.2
0.1
1.2
1.4
1.6
2.0
RED LINE GROWTH RATE
WIND RADIUS / STELLAR RADIUS
1.8
1.6
1.4
1.2
1.0
.8
.6
.4
.2
0
-.2
1.0
2.0
3.0
4.0
5.0

Figure 5